Supporting Information

Red-Emissive Nanocrystals of $Cs_4Mn_xCd_{1-x}Sb_2Cl_{12}$ Layered Perovskite

Emanuela Sartori,[a,b] Marta Campolucci,[a,b] Dmitry Baranov,[b] Min Zeng,[c,d] Stefano Toso,[b,e] Giorgio Divitini,[f] Maurizio Ferretti,[a] Zeger Hens,[d] Liberato Manna,[b] Federico Locardi[a,b,d,*]

a Department of Chemistry and Industrial Chemistry, Università degli Studi di Genova, Via Dodecaneso 31, 16146 Genova, Italy
b Nanochemistry Department, Istituto Italiano di Tecnologia, Via Morego 30, 16163, Italy
c Hubei Key Laboratory of Ferro- & Piezoelectric Materials and Devices, Faculty of Physics and Electronic Science, Hubei University, Wuhan, 430062, P. R. China
d Physics and Chemistry of Nanostructures group (PCN), Ghent University, Krijgslaan 281, Gent 9000, Belgium
e International Doctoral Program in Science, Università Cattolica del Sacro Cuore, 25121 Brescia, Italy
f Electron Spectroscopy and Nanoscopy, Istituto Italiano di Tecnologia, Via Morego 30, 16163, Italy

Experimental Procedures

Chemicals. Cesium carbonate (Cs_2CO_3, 99%), manganese (II) acetate ($Mn(OAc)_2$, 98%), cadmium (II) acetate ($Cd(OAc)_2$, 99.99%), antimony (III) acetate ($Sb(OAc)_3$, 99.99%), oleic acid (OA, technical grade, 90%), dioctyl ether (DOE, technical grade, 99%), benzoyl chloride (Bz-Cl, 99%), ammonium thiocyanate (Amm-Thioc, technical grade, 97.5%), cadmium (II) chloride ($CdCl_2$, 99.99%), didodecyldimethylammonium chloride (DDAC, 98%) toluene and hexane were purchased from Sigma Aldrich. Oleylamine (OlAm, technical grade, 80-90%) was purchased from Fisher Scientific. All chemicals were used as received without further purification.

Synthesis of $Cs_4Mn_xCd_{1-x}Sb_2Cl_{12}$ Nanocrystals (NCs). $Cs_4Mn_xCd_{1-x}Sb_2Cl_{12}$ NCs ($0 < x < 1$) were synthesized by a hot-injection method. Samples with different Mn^{2+} (and Cd^{+2}) concentrations were obtained by changing the Mn^{2+} (and Cd^{2+}) precursor amounts during the synthesis. The compositions explored were x = 0, 0.1, 0.15, 0.20, 0.25, 0.30, 0.40, 0.50, 0.60, 0.70, 0.80, 0.90 to 1.00 (feeding ratios, expressed as $Mn^{2+}/(Cd^{2+} + Mn^{2+})$ in moles). In a typical synthesis, the precursors Cs_2CO_3 (81.5 mg, 0.355 mmol), $Mn(OAc)_2$ (21.6 mg, 0.125 mmol), $Cd(OAc)_2$ (33.3 mg, 0.125 mmol), and $Sb(OAc)_3$ (74.7 mg, 0.250 mmol) were mixed with OA (2.00 mL), OlAm (0.875 mL) and DOE (4.00 mL) in a 50 mL three-neck flask. The mixture was stirred at 115 °C under vacuum for 20 min, and once all precursors were dissolved, the mixture was heated to 160 °C in N_2 atmosphere. Before the injection, the color of the solution was light yellow. Then, 0.400 mL of Bz-Cl in 0.400 mL of DOE were injected, and the solution quickly turned turbid and beige. Immediately after the injection, the solution was cooled down in an ice bath. To recover the particles, the mixture was centrifugated for 5 min at 4500 rpm. The resulting precipitate was centrifuged again for 2 min at 4500 rpm in order to eliminate the remaining ligands, and then dispersed in 4 mL of hexane. The final solution was centrifuged for 5 min at 4500 rpm, and the clear supernatant containing the NCs was collected for further characterization.

Post-synthesis treatment of $Cs_4Mn_{0.12}Cd_{0.88}Sb_2Cl_{12}$ Nanocrystals (NCs). To investigate the possibility of increasing the quantum yield of as-synthesis NCs, we performed three different post-synthesis treatments.

Ammonium thiocyanate (NH_4SCN). In a 20 mL vial, 1 mL of Mn 12% sample (prepared as described above) and 80 mg of NH_4SCN were stirred in 3 mL of hexane at room temperature for 3 hours. Starting 30 minutes after the beginning, an aliquot of 250 µL has been taken every 15 minutes and centrifuged at 2000 rpm for 3 min to recover the treated particles. The precipitate was discarded, while the supernatant was kept and analyzed.

Cadmium chloride ($CdCl_2$). The treatment with $CdCl_2$ consisted in mixing 0.1 mmol of $CdCl_2$ in 100 µL of OA, 100 µL of OlAm, 3 mL of hexane for 1 hour at ~70 °C. Then, 500 µL of the 12% Mn sample were added at room temperature. Aliquots of 300 µL have been taken and analyzed at different times, as reported in Table S2.

Didodecyldimethylammonium chloride (DDAC). 0.05 mmol of DDAC were solubilized in 5 mL of toluene. Increasing amounts of this solution were added to a suspension of 3 µL of the Mn 12% sample diluted in 3 mL of toluene. An aliquot was taken and analyzed 5 min after each addition.

Inductively Coupled Plasma (ICP) Elemental Analysis. The ICP elemental analysis was carried out *via* inductively coupled plasma optical emission spectroscopy (ICP-OES) with an iCAP 6300 DUO ICP-OES spectrometer (ThermoScientific). All chemical analyses performed by ICP-OES were affected by a systematic error of about 5%. For the analyses, 20 µL of the sample were dissolved in 0.625 mL of hydrochloric acid (HCl 37%) and 1.875 mL of nitric acid (HNO_3 60% v/v), diluted using 20 mL of Milli-Q water. Then, an overnight digestion was needed to proceed with dilution to 25 mL and filtration by a 0.45 µL filter.

UV–Vis absorption, Photoluminescence (PL), PL lifetime and PL Quantum Yield (QY) Measurements. The optical absorption spectra were measured using Cary 300 spectrophotometer and normalized at 250 nm for plotting. The spectra were recorded in 10 mm pathlength quartz cuvettes, filled with solutions prepared by diluting 3 µL of nanocrystal dispersion in 3 mL of anhydrous hexanes. The measured OD at 250 nm varied from ~0.75 to ~1.5.

The PL and PLE spectra were measured using an Edinburgh FLS920 spectrofluorometer in 90 degrees geometry, equipped with a Xe lamp as an excitation source. The PL spectra were measured at 320 nm excitation (excitation slit width 5 nm, emission slit width 2 nm) and, for a comparison across samples with different optical density, were scaled by transmittance at the excitation wavelength: $PL'(\lambda) = PL(\lambda)/[1-T(320\ nm)]$, where $T(320\ nm) = 10^{-Abs(320\ nm)}$. The PLE spectra were measured at the PL maximum (excitation slit width 2 nm, emission slit width 10 nm) and, for a comparison across samples of different optical density, were scaled by a spectral transmittance: $PLE'(\lambda) = PLE(\lambda)/[1-T(\lambda)]$, where $T(\lambda) = 10^{-Abs(\lambda)}$. The PLQY was measured using an integrating sphere and 320 nm excitation (10 nm excitation slit width and 0.8 nm detection slit width).

Powder X-ray diffraction (XRD) measurements. The XRD analysis was performed on a PANanalytical Empyrean X-ray diffractometer, operating at 45 kV and 40 mA and equipped with a 1.8 kW CuKα ceramic X-ray tube and a PIXcel3D 2 ×2 area detector. The samples were prepared by concentrating

the NC solutions by solvent evaporation and then drop-casting them onto a silicon zero-diffraction single crystal substrate. The diffraction patterns were collected in a parallel beam geometry and symmetric reflection mode under ambient conditions, in the range 10 – 90 2theta°, with a scanning step of 0.02°. XRD data analysis were analyzed using the HighScore 4.1 software from PANalytical.

Transmission electron microscopy (TEM) measurements. Bright-field TEM (BF-TEM) imaging was performed on a JEOL JEM-1011 microscope equipped with a thermionic gun operating at 100 kV. For the analyses, the samples have been diluted and drop-casted onto carbon-coated 200 mesh copper grids. The mean size was calculated using the Fiji software on at least 300 NCs; agglomerates outside the range 5 – 20 nm were not taken into account. High-Resolution STEM imaging was carried out on a probe-corrected ThermoFisher Spectra 300 STEM operated at 300 kV, acquiring the high angle annular dark field (HAADF) signal. Energy-Dispersive X-ray (EDX) signal was collected using a Dual-X detector using a probe current of 150 pA. Data were acquired and processed using Velox. Samples for HRSTEM were deposited on copper grids with ultrathin carbon.

Table S1. Experimental ratio (%) $[Mn^{2+}/(Cd^{2+}+Mn^{2+})]*100$ of $Cs_4Mn_xCd_{1-x}Sb_2Cl_{12}$ NC samples measured via ICP-OES.

$Mn^{2+}/(Cd^{2+}+Mn^{2+})*100$ theoretical	$Mn^{2+}/(Cd^{2+}+Mn^{2+})*100$ experimental
0	0
10	6.3
15	9.2
20	11.5
25	10.5
30	15.3
40	16.6
50	34.9
60	38.2
70	51.0
80	66.9
90	82.1
100	99.9

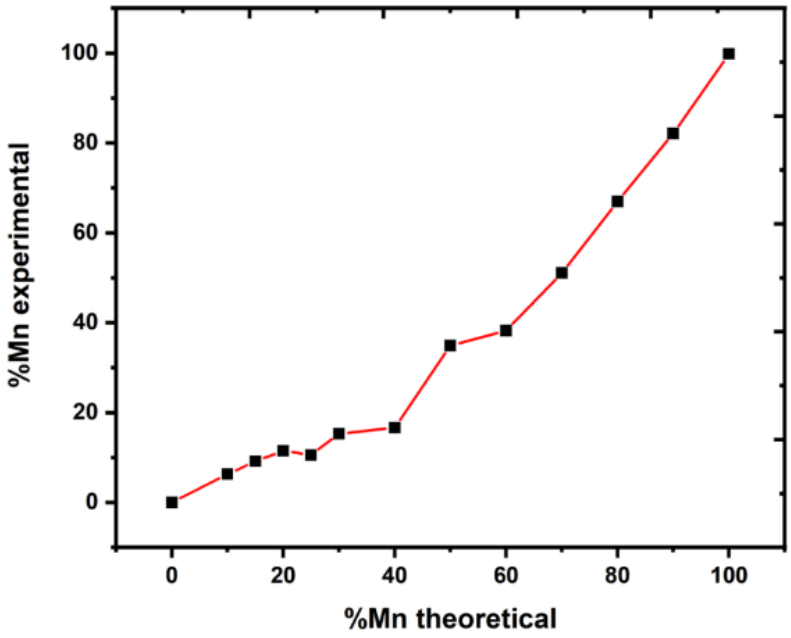

Fig. S1. Experimental ratio $[Mn^{2+}/(Cd^{2+}+Mn^{2+})]*100$ vs theoretical one of $Cs_4Mn_xCd_{1-x}Sb_2Cl_{12}$ NC samples.

The amount of Mn^{2+} in the nanocrystals was found to be smaller than the feeding ratio. The change of slope observed in Fig. S1 indicates that the inclusion of Mn^{2+} is less efficient for higher Cd^{2+} concentration (Mn^{2+} feeding ratio < 50%).

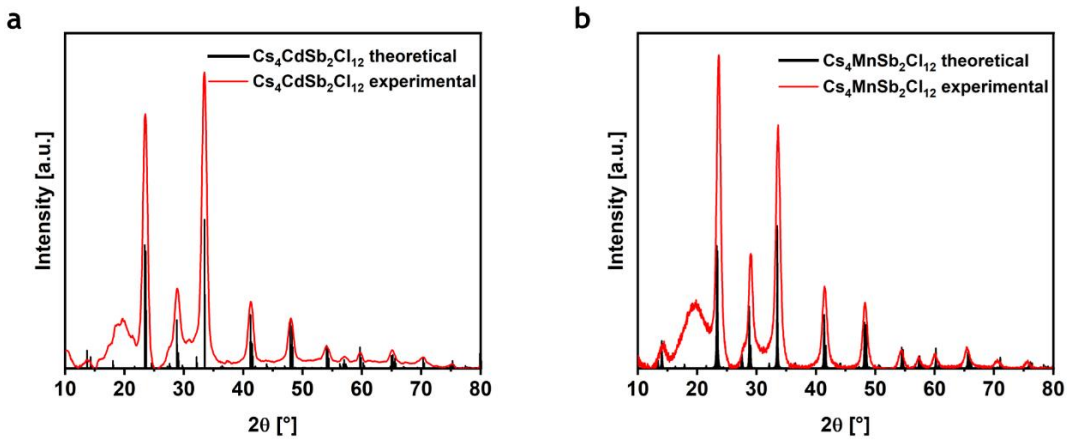

Fig. S2. (a) Comparison between theoretical and experimental pattern of $Cs_4CdSb_2Cl_{12}$. (b) Comparison between theoretical and experimental pattern of $Cs_4MnSb_2Cl_{12}$.

We investigated the dependence of the unit cell parameters on the Mn^{2+}/Cd^{2+} ratio in the sample. First, we measured the peak position of the five most intense peaks in the diffractogram (2θ ≈ 23.5°; 29.0°; 33.5°; 41.5°; 48.3°) by fitting them with a gaussian profile. The peaks were indexed according to the published reference structure ICSD-14995[1]: (110)+(018); (024); (208); (300)+(128)+(1016); (220)+(2016). Second, we converted the peak position from the 2θ to the scattering vector q = $4\pi \cdot \sin(\theta)/\lambda_{XRD}$ scale. We then exploited the fact that the *q* positions of peaks with Miller indices multiple of each other are linear in the *q* scale to apply a q-shift for correcting small misalignments of the diffractometer. Finally, we extracted the unit cell parameters for each diffractogram by minimizing the average difference between the $1/d(hkl)^2$ values measured experimentally from each peak and the value calculated according to the equation for the hexagonal system:

$$\frac{1}{d(hkl)^2} = \left[\frac{4}{3}(h^2 + k^2 + hk) + l^2\left(\frac{a}{c}\right)\right] \cdot \frac{1}{a^2}$$

The process was repeated for each sample, and results are summarized in Fig. S3.

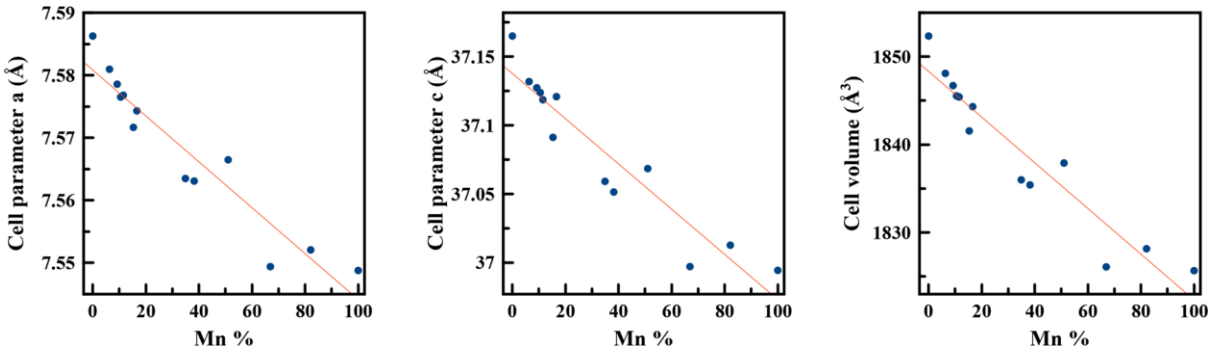

Fig. S3. Evolution of the unit cell parameters *a* (left), *c* (center) and of the unit cell volume (right) with the Mn^{2+} content of the sample. The red straight lines are meant as a visual aid.

The relatively high uncertainty in the determination of the unit cell parameters is due to the broadening of diffraction peaks and to the overlap of close reflections. However, the decrease in the unit cell parameters and volume with increasing Mn^{2+} content is well visible.

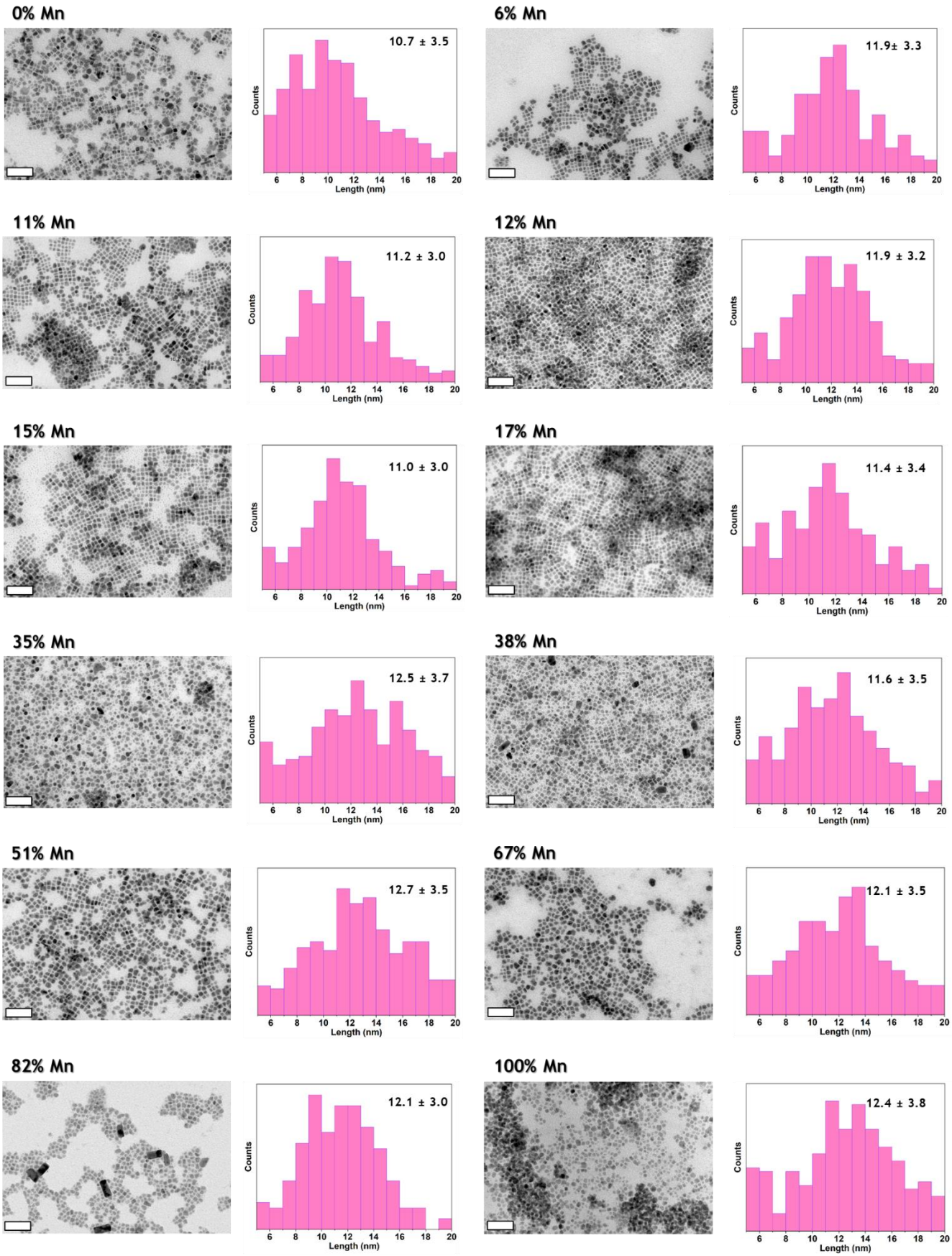

Fig. S4. TEM micrographs of $Cs_4Mn_xCd_{1-x}Sb_2Cl_{12}$ NCs together with the corresponding size distribution histograms. The scale bars are 100 nm.

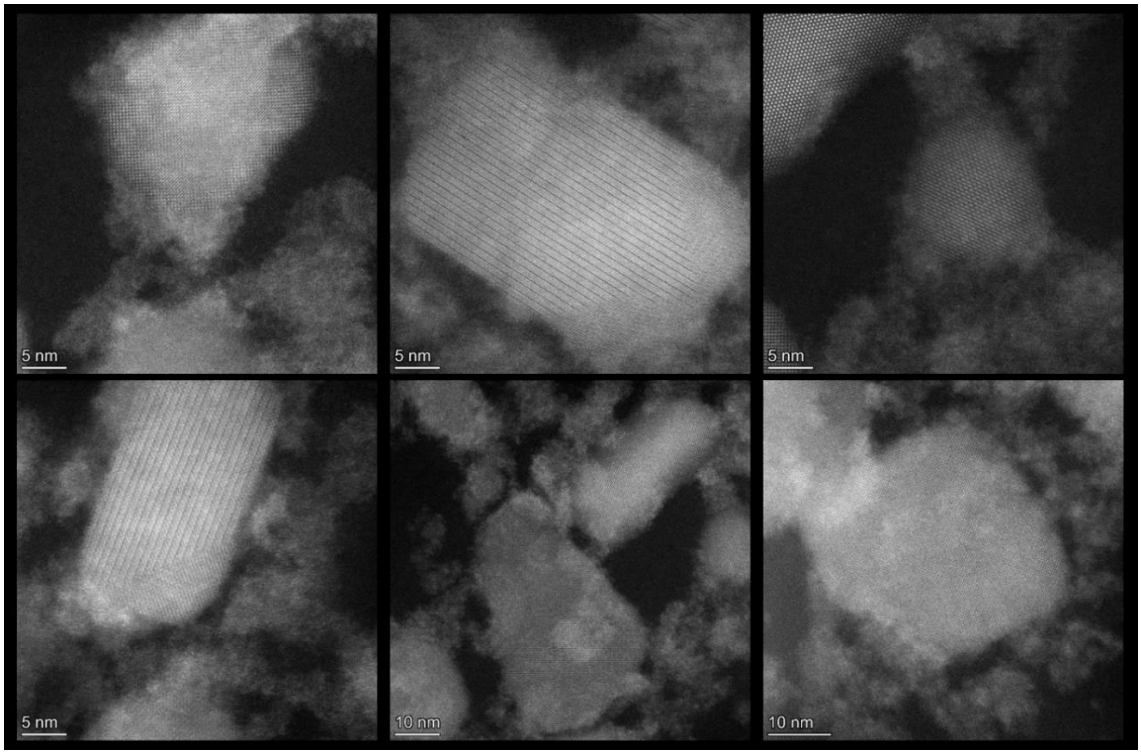

Fig. S5. HAADF-STEM images of several NCs. Larger particles preserve the crystallinity and occasionally become polycrystalline.

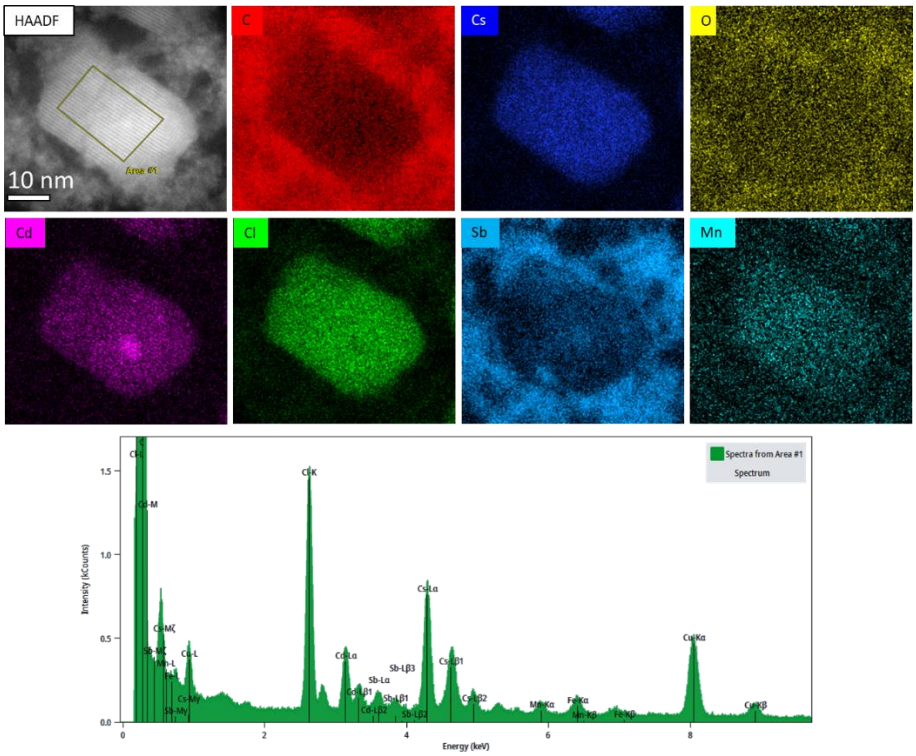

Fig. S6. HAADF-STEM image and elemental maps for a single nanocrystal. The EDX spectrum was collected across the area within the yellow rectangle, and is representative of the average composition of the nanocrystals. All the expected elements were observed within the particles. A segregation of Sb at the edge of the NCs was observed, in addition to the Sb contained inside. The Cu signal is spurious and originates from the TEM support grid.

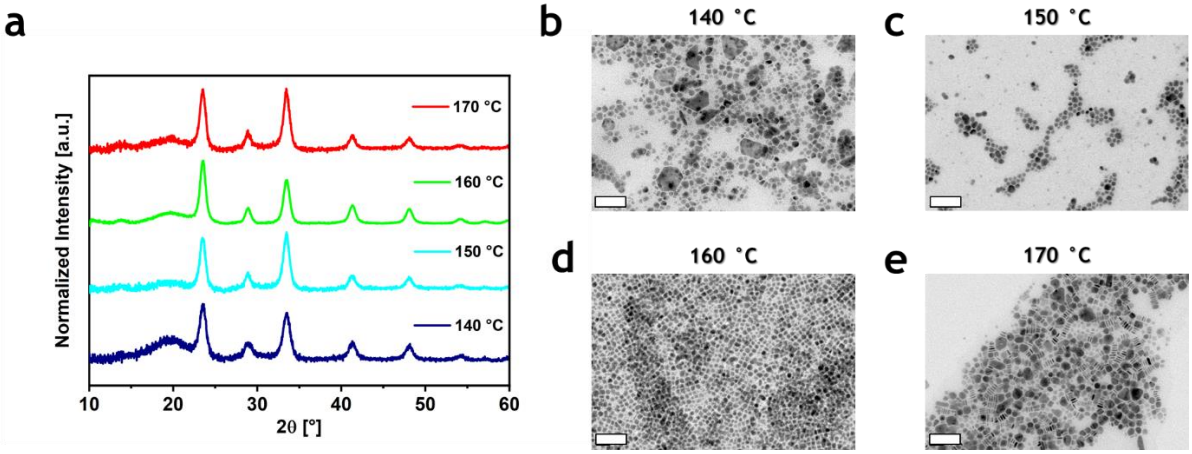

Fig. S7. (a) Comparison between the XRD patterns of the sample $Cs_4Mn_{0.12}Cd_{0.88}Sb_2Cl_{12}$ synthesized at four different temperatures: 140 °C – 150 °C – 160 °C – 170 °C. (b-e) TEM micrographs of the corresponding samples.

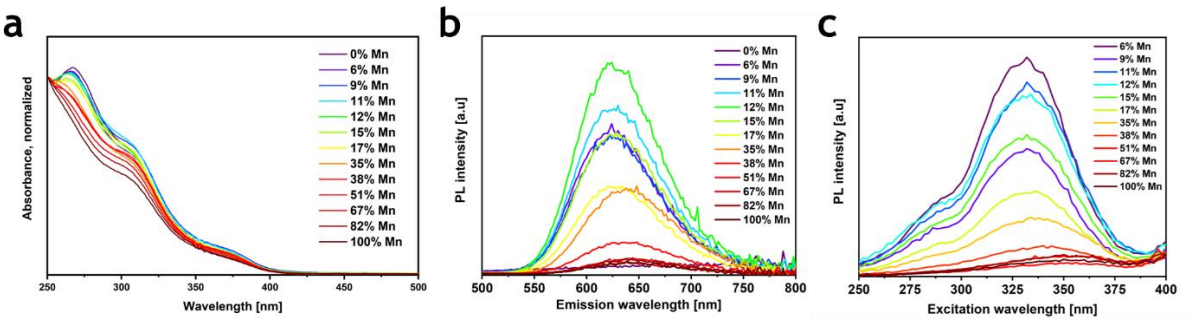

Fig. S8. (a) Normalized optical absorption at 250 nm of all the series $Cs_4Mn_xCd_{1-x}Sb_2Cl_{12}$. (b) Corresponding PL spectra corrected for 1-T (transmittance) of all the series $Cs_4Mn_xCd_{1-x}Sb_2Cl_{12}$, excitation wavelength 320 nm; (c) Respective PLE spectra collected at the PL maximum.

Table S2. Different aliquots analyzed for monitoring the post – synthesis treatment. The time, in minutes and second for NH_4SCN and $CdCl_2$ respectively, or the volume of the DDAC solution added, indicate the conditions after which each aliquot was taken and analyzed.

Aliquot	Treatment with NH_4SCN	Treatment with $CdCl_2$	Treatment with DDAC
1	30 min.	30 sec.	10 μL
2	45 min.	60 sec.	15 μL
3	60 min.	90 sec.	20 μL
4	75 min.	120 sec.	25 μL
5	90 min.	150 sec.	30 μL
6	105 min.	300 sec.	40 μL
7	120 min.	420 sec.	80 μL
8	135 min.	540 sec.	
9	150 min.		
10	165 min.		
11	180 min.		

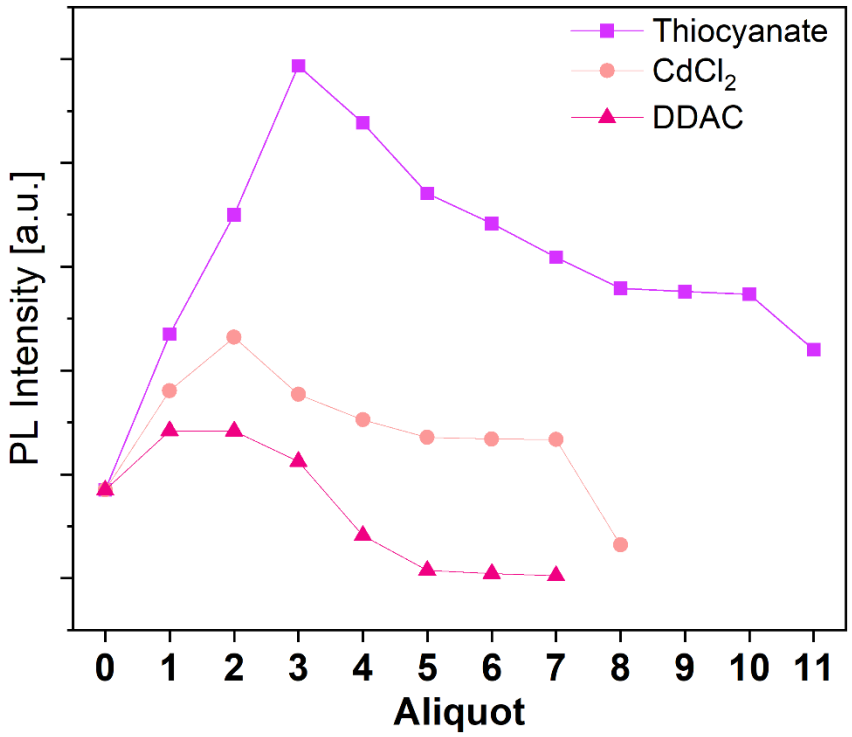

Fig. S9. Variation of the PL intensity of the $Cs_4Mn_{0.12}Cd_{0.88}Sb_2Cl_{12}$ sample during the different treatments.

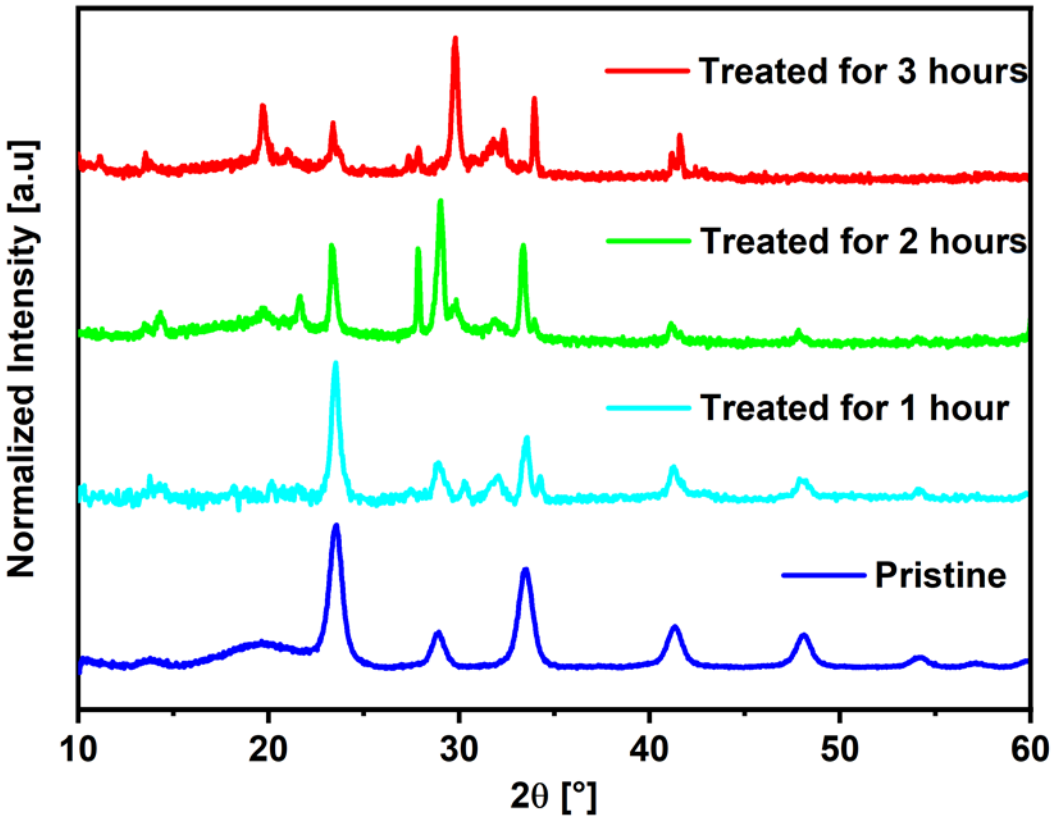

Fig. S10. Comparison between the XRD patterns of the sample $Cs_4Mn_{0.12}Cd_{0.88}Sb_2Cl_{12}$ before and after the post-synthesis treatment with ammonium thiocyanate for 1 – 2 – 3 hours.

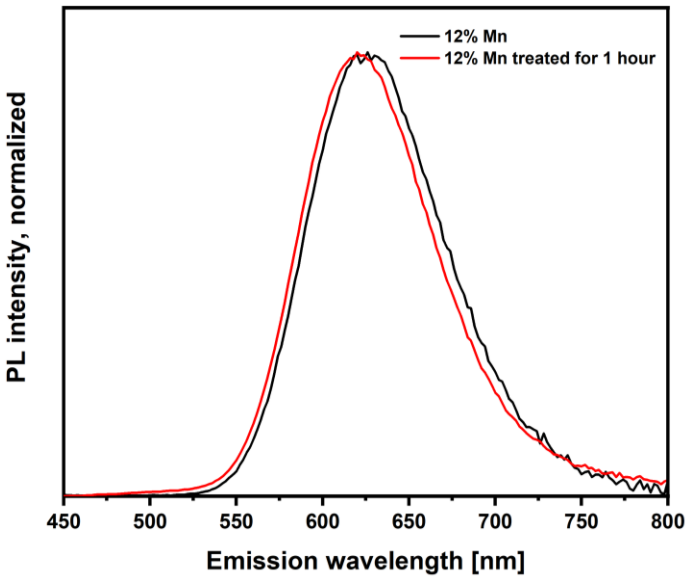

Fig. S11. Normalized PL of $Cs_4Mn_{0.12}Cd_{0.88}Sb_2Cl_{12}$ before (black line) and after thiocyanate treatment (red line).

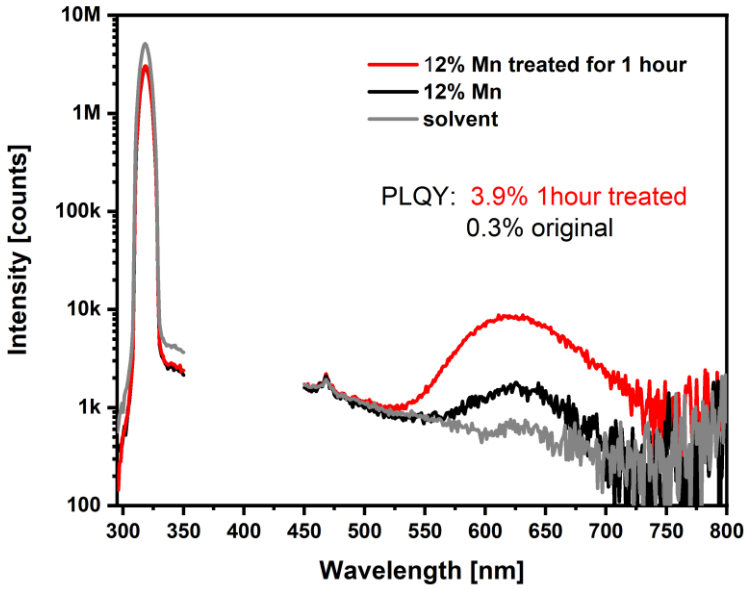

Fig. S12. PLQY of the 1 hour-treated $Cs_4Mn_{0.12}Cd_{0.88}Sb_2Cl_{12}$ sample is 3.9%, vs 0.3% for the untreated sample.

References

1 B. Vargas, R. Torres-Cadena, D. T. Reyes-Castillo, J. Rodríguez-Hernández, M. Gembicky, E. Menéndez-Proupin and D. Solis-Ibarra, *Chem. Mater.*, 2020, **32**, 424–429.